

# Droplet Cluster Behavior in Dense and Dilute Regions of a Spray

J. Bellan

Jet Propulsion Laboratory  
California Institute of Technology  
Pasadena, CA 91109

## 1 INTRODUCTION

concern regarding the efficiency, stability and safety margins of hi-propellant combustion in rocket engines has prompted the investigation of many specific aspects of spray evaporation, ignition and combustion previously not studied. Thus, early studies of combustion in liquid rocket engines were based upon the results of the classical single-component, isolated drop combustion at atmospheric pressure<sup>1</sup>. Although the results from these studies provided a baseline for understanding some of the phenomena occurring in liquid rocket engines, they fail to explain important observations and facts obtained from examining rocket performance after many flights. Examples are the loss of about 3% of the liquid oxygen ( $LO_x$ , one of the propellants) which exits unburned<sup>2</sup>, and the existence of striations on the inner wall of engines examined after a flight<sup>3</sup>. It then becomes apparent that many significant issues of liquid rocket spray combustion were not addressed by the early models and that in order to mitigate existing problems, it is necessary to understand aspects previously unexplored. Since characterization of combustion in liquid rocket chambers is extremely difficult due to the lack of diagnostics operating under such harsh condition<sup>3</sup>, the strategy has been to infer the relevant aspects to be studied from laboratory experiments bearing similarity to liquid rocket combustion chambers. Such experiments have focussed generally on a single poorly-understood aspect of liquid rocket chamber combustion so as to isolate the fundamental effects of this aspect before coupling it to the other phenomena.

The phenomenology of hi-propellant spray evaporation, ignition and combustion in a highly turbulent environment at elevated pressure (supercritical with respect to the fuel) is as follows: When oxygen and hydrogen enter the combustion chamber, due to the higher critical temperature of oxygen with respect to that of hydrogen, the drops of hydrogen quickly become a fluid whereas the drops of oxygen remain liquid. Thus, the relevant phenomena to be studied are the evaporation of  $LO_x$  drops in surroundings initially composed of fluid  $H_2$ , the eventual transition of  $LO_x$  drops to a fluid, ignition of the fluid mixture and the subsequent combustion. Due to the supercritical conditions, volatility of  $H_2$  into  $LO_x$  becomes important, so that although the two component fuels are initially separated, very rapidly the liquid drops become composed of a binary-fuel. Since the concentration of the drops varies in time, the critical point of the fuel inside the drops is also a function of time. Therefore, during evaporation and solvation, the critical point may be crossed back and forth as the composition of the fuel changes. The same comments apply to tri-propellant liquid rocket engine phenomenology where an additional

fuel, *RP1*, may be used in the initial combustion stage in series or in parallel with the bi-propellant in order to maximize the margin of engine operation. *RP1* is a mixture of long chain hydrocarbons which has basic properties similar to those of kerosene. Thus, hydrocarbon solubility into LO. drops is of interest, as the liquid inside the drops will become a multicomponent mixture.

## 2 BEHAVIOR OF CLUSTERS OF MULTICOMPONENT FUEL DROPS IN AIR AT ATMOSPHERIC PRESSURE: MODELING AND RESULTS

In order to address the multicomponent feature discussed above, investigations of the evaporation, ignition and combustion of clusters of binary-fuel drops were conducted. The choice of the binary system was motivated by the difficulty of following the behavior of a multitude of components in practical calculations, as well as by the interest of unraveling the relative behavior of solvent and solute when drop interactions are important. Although the studies described here were performed at atmospheric pressure, they represent a first step toward the general goal of understanding the role of the two components during evaporation, ignition and combustion of collections of drops.

Generally, solvent and solute are characterized relative to each other as follows: The solvent is the less volatile, more viscous component of the fuel and the solute is the more volatile, less viscous component of the fuel. However, "volatility" is an engineering term which does not have a precise physical definition. High volatility is associated both with a low normal boiling point and with a small latent heat of evaporation. When two components such as *n*-decane and *n*-hexane are considered, it is difficult to decide which is the solvent and which is the solute because the normal boiling point of *n*-decane is higher than that of *n*-hexane but its latent heat of evaporation is lower. In the following, we present results from studies of clusters of binary-fuel drops showing that the normal boiling point and the latent heat are each important for defining volatility, but in different cluster regimes. Moreover, we will also discuss why liquid mass diffusion is important during the evaporation of the solute in the dilute cluster regime, in agreement with the isolated drop theories, and why it does not play a major role in the evaporation of drops in dense clusters, except during the very initial stage.

### 2.1 Evaporation of binary-fuel drops in clusters

Studies of binary-fuel isolated drops<sup>4</sup>, have identified liquid mass diffusion as the driver of solute evaporation when there is a slip velocity around a binary-fuel drop is exposed to a flow. Under quiescent conditions, liquid mass diffusion does not play an important role in the evaporation of the solute because its characteristic time is much larger than the drop lifetime. However, under convective conditions, the slip velocity at the surface of the drop induces through surface shear a circulatory motion inside the drop in the form of Hill vortices. This circulatory motion enhances liquid mass diffusion, its characteristic time becomes accordingly reduced and of comparable magnitude to that of the drop lifetime. It is under these conditions that liquid mass diffusion becomes important in bringing solute from the drop core to the surface and preferentially inducing its evaporation.

Experimental observations of burning and nonburning sprays at atmospheric pressure have revealed that drops tend to cluster. In burning sprays, a single flame has been found to enclose each cluster, thus indicating important drop interaction. This drop interaction has been quantified by Bellan and Harstad<sup>5</sup> through the concept of the "sphere of influence" around each drop of the cluster. For single-size clusters of drops, each sphere

of influence is centered at the center of a drop and has for radius the half distance between the centers of adjacent drops; the nondimensional radius of the sphere of influence,  $R_2$ , is the ratio of the radius of the sphere of influence to the drop radius,  $R$ . Since by definition the spheres of influence are tightly packed in the cluster volume, this volume is composed of the ensemble of all spheres of influence and the spaces between the spheres of influence. The cluster surface is the envelope of the spheres of influence. This definition of the sphere of influence allows to account for drop interaction through the magnitude of the nondimensional radius of the sphere of influence. For  $R_2 \leq 10$ , the evaporation time may be twice that of the isolated drop; the cluster is then called "very dense". When  $10 < R_2 \leq 15$ , the evaporation time may be approximately 50% larger than that of the isolated drop; the cluster is then called "dense". For  $15 < R_2 \leq 30$ , the evaporation time may be at most 10% larger than that of the isolated drop; the cluster is then called "dilute". Finally, for  $R_2 > 30$ , the evaporation time tend.. toward an asymptote; the cluster is called then "very dilute".

According to whether the cluster evaporates in any of these four configurations, the results obtained for the isolated drop evaporation might hold or not. This was discussed by Harstad and Bellan<sup>6</sup> who studied the behavior of a spherical cluster of binary-fuel drops at atmospheric pressure when the solute is much more volatile than the solvent. The gas inside the cluster was initially at rest whereas the drops initial velocity,  $u_d^0$ , was non null; as the drops moved, they entrained the gas which acquired a velocity of its own. A number,  $Be \equiv -[R/(D_m u_l)]^{0.5} dR/dt$  ( $D_m$  is the mass diffusivity,  $u_l$  is the circulatory velocity inside the drop and  $t$  is the time), was defined representing the ratio of the drop mass regression rate to a characteristic solute diffusion rate. Thus, when  $Be \ll 1$ , diffusion into the boundary layer governs the rate of solute transfer from the liquid core to the drop surface and evaporation from the surface occurs at a rate defined by the Langmuir-Knudsen evaporation law. Since the two processes are sequential, it is in fact the slower of these two rates which governs evaporation. In contrast, when  $Be \gg 1$ , the transfer of solute from the liquid core to the gas phase is governed by surface layer stripping, that is by the regression rate of the drop. The reader is referred to Harstad and Bellan<sup>6</sup> for the details of the model. Figure 1 reproduced from Harstad and Bellan<sup>6</sup> shows the variation of  $Be$  with the residual drop radius,  $R_1$ , defined as the ratio of the drop radius to the initial drop radius, for an extended range of initial air/fuel mass ratios,  $\Phi^0$ 's, corresponding to an extended range of values of  $R_2^0$  (as  $R_2^0$  is a monotonically increasing function of  $\Phi^0$ ).  $T_{ga}^0$  is the initial gas temperature in the cluster which is taken to be that of the gas surrounding the cluster;  $Y_{Fva}^0$  is the initial fuel mass fraction in the cluster gas which is taken to have the same value as that in the gas surrounding the cluster;  $T_{gs}^0$  is the initial temperature of the drop, assumed uniform;  $Y_{VL}^0$  is the initial mass fraction of the solute in the drop core; and  $R_c^0$  is the initial cluster radius. The plots in Fig. 1 show that in the very dense and dense regimes, although  $Be$  is  $O(1)$  initially, it quickly becomes  $\gg 1$  during the drop lifetime. In contrast, in the dilute and very dilute regimes  $Be$  is  $O(1) - O(10)$  during the entire drop lifetime. This is due to the different drop dynamics in dense and dilute clusters of drop: a denser cluster exposes more area to the flow and thus the drag force is stronger. This results in a quicker relaxation of the slip velocity between phases,  $\vec{u}_s$ ; consequently, the shear at the drop surface decays very fast during the drop lifetime, and  $u_l$  becomes accordingly small. As the regression rate of the drop is smaller than the decay of  $u_l$  because drop heating is hindered by the presence of other drops in close proximity,  $Be$  becomes  $\gg 1$ . Plots of the mass fraction of the solute in the drop core,  $Y_{VL}$ , versus  $R_1$  shown in Fig. 2 (also reproduced from Harstad and Bellan<sup>6</sup>) concur with this physical picture: except for an initial effect of the liquid mass diffusion which decreases the solute mass fraction as it is preferentially vaporized, its value remains constant inside the drop showing that it evaporates at the rate of the solvent.

When the initial drop velocity is increased by a factor of 5, these results remain valid in the very dense and dense regimes, however, in the dilute and very dilute regimes the influence of liquid mass diffusion is present during the major portion of the drop lifetime and the value of the solute mass fraction continues to decrease with  $R_1$ . This is depicted in Fig. 3 reproduced from Harstad and Bellan.<sup>6</sup> These results support the above physical interpretation.

## 2.2 Ignition of binary-fuel drops in clusters

The study of binary-fuel drop ignition in clusters performed by Bellan and Harstad<sup>7</sup> is based upon the assumption that the chemistries of solvent and solute are independent. Thus, two Damköhler numbers are defined, and the criterion derived by Law and Chung<sup>8</sup> and previously used for clusters of single-component drops<sup>9</sup> is expanded to account for the ignition of the two components. According to this criterion which is consulted at every time step of the calculation, the component whose Damköhler number is larger than the respective ignition Damköhler number initiates ignition. Once ignition occurs, the location of the flame is calculated as in Bellan and Harstad.<sup>9</sup>

The ignition location is found to be always outside the cluster except for situations where  $R_2^0 > 34$  (the very dilute regime) and the initial mass fraction of solute is very small (2%). For the baseline set of parameters chosen in Bellan and Harstad<sup>7</sup>, ignition did not occur in the very dense regime. When the kinetic parameters are identical for the two components, in the part of the dense regime adjacent to the very dense regime ignition is always initiated by the solvent, whereas in the very dilute regime ignition is always initiated by the solute. Between the solvent-controlled and the solute-controlled regimes, there exists a range where control is entirely dominated by the relative kinetics of the two compounds. For the hypothetical case of identical kinetics, the solvent and solute alternately initiate ignition as  $\Phi^0$  increases; however, as ignition of the igniting compound is artificially suppressed by nulling the respective preexponential constant, the other compound initiates ignition at same time and  $R_1$  thereby showing that there is no true control by either one of the compounds. In contrast, if the same artifact is used to suppress ignition for the smallest  $\Phi^0$  for which ignition is obtained, no ignition occurs. When the above artifact is used to suppress ignition by the solute for the largest  $\Phi^0$  considered in Bellan and Harstad<sup>7</sup>, physically incorrect results are obtained (mass fraction related parameters in the ignition Damköhler number become negative). These simple exercises show that it is indeed the solvent that controls ignition for the smallest  $\Phi^0$ , and it is indeed the solute that controls ignition for the largest  $\Phi^0$ . These results are a consequence of the evaporative behavior dominated by the solvent in the very dense regime and by the solute in the very dilute regime. Figures 4 and 5 reproduced from Bellan and Harstad<sup>7</sup> illustrate these results.

To physically understand what determines the ignition time it is instructive to consider two competing processes and their characteristic times. The first is the relaxation of the slip velocity,  $\mathcal{R}_1$ , and the second is the rate at which the Damköhler number approaches the respective ignition Damköhler number of the compounds,  $\mathcal{R}_{2,i}$ , where  $i$  refers to the compound. If  $\mathcal{R}_1 > \mathcal{R}_{2,i}$ , then  $Be$  becomes very large by the time ignition occurs and then the solvent controls ignition. In the opposite case ignition occurs very fast with respect to the relaxation rate of  $\vec{u}_s$ ,  $Be$  remains relatively small, and thus the solute controls ignition.

Interesting insights can be obtained by considering the respective roles of solute and solvent identity. Thus, calculations were performed with No.2 GT fuel as solvent and with n-decane, n-hexane and n-heptane as solutes; the initial mass fraction of the solute was 0.2 in all cases. Both n-hexane and n-heptane have larger latent heats and higher saturation

pressures than n-decane. N-hexane has a larger latent heat and a higher saturation pressure than n-heptane. Despite all these differences in properties, the results show negligible variations in the ignition time and associated residual radius. Such a result is expected in the very dense regime since the solute is not controlling. What the results indicate is that the effects of the latent heat and saturation pressure are balanced, so that the solute identity does not influence ignition even in the very dilute regime. A very different picture emerges when one considers the effect of the solvent. Figure 6 depicts results obtained with No.2 GT and n-decane as solvents (n-decane has both a larger latent heat and a larger saturation pressure than No.2 GT fuel) and n-hexane as solute. Replacing No.2 GT with n-decane has suppressed ignition for the smallest  $\Phi^0$  thus indicating that the effect of latent heat dominates that of the saturation pressure when the drops are in close proximity. This is consistent with the evaporative behavior of dense clusters of drops which is limited by the availability of heat to the drops. As the latent heat is increased, the situation is exacerbated and ignition is prevented. However, the range of strongly-controlled solvent ignition extends now farther, to larger values of  $\Phi^0$  and  $R_2^0$ . This is because for a given value of  $\Phi^0$  the cluster has now stronger dense characteristics since the latent heat of the solvent is larger. Examination of the ignition characteristics in the very dilute regime reveals that ignition occurs earlier when n-decane is the solvent; this is attributed to the larger saturation pressure which plays a dominant role when evaporation is no longer limited by drop heating. Although ignition occurs earlier in time, it occurs later in the drop lifetime because evaporation is faster due to the higher saturation pressure. Thus, the conclusion is that it is the latent heat of a fuel that determines its volatility in the very dense regime whereas it is its saturation pressure that determines its volatility in the very dilute regime. Both properties play a role in the intermediate regimes.

### 2.3 Cluster combustion of binary-fuel drops

For single-component fuel drops it has been shown that cluster flames exist only in a restricted range of values of  $\Phi^{010}$ . This is because if  $\Phi^0$  is very small, the cluster is so dense that the drops extract too much heat from the gas during evaporation, before heat transfer from the cluster surroundings may replenish it; thus, the temperature becomes too low to initiate ignition. In contrast, if  $\Phi$  is very large at ignition, the gaseous mixture inside the cluster is fuel-lean and internal flash combustion depletes all gaseous fuel inside the cluster; with no gaseous fuel left to escape the cluster, the external cluster flame cannot become established. These two situations represent the lower and upper limits for the existence of cluster flames.

The model of binary-fuel drop cluster combustion is an extension of the model of Bellan and Harstad<sup>10</sup> to binary fuels: (1) for the internal flash flame, the oxygen inside the cluster is apportioned between solvent and solute according to their average mass fractions at ignition, and (2) the component initiating ignition determines the flame standoff distance from the cluster and the two components burn stoichiometrically at the flame.

The situations studied are all identified in Table 1 and the symbols correspond to those in Figs. 7-12. Figures 7, 8 and 9 display the fractions of solvent and of solute burnt in the flash flame following ignition and the ratio of these fractions. The fractions are increasing functions of  $\Phi^0$  because although for larger  $\Phi^0$ 's ignition occurs earlier in the drop lifetime, there is more oxygen inside the cluster and thus more of the fuel can burn. Note that the ratio of the fractions is always smaller than  $Y_{VL}^0 / (1 - Y_{VL}^0)$  and is constant with  $\Phi^0$ . The reason for this is the initially larger relative velocity at the drop surface which preferentially evaporates the solute (this i.e. the  $Be \ll 1$  regime). As a result,  $Y_{VL}$  decreases. Since  $\vec{u}_s$  decreases because of drag effects, eventually  $Be \gg 1$ . Then, the

preferential evaporation of the solute ceases and the solute evaporates at the rate of the solvent, that is at the frozen rate corresponding to the mass fraction when  $Be$  became  $\gg 1$ . This physical picture is the result of examining  $Be$  and the fractional evaporation rate of the solute,  $\dot{m}_v/\dot{m}$ , versus the residual drop radius,  $R_1$ . Additionally, this is confirmed by results showing that the ratio of the flash flame burn fractions is a decreasing function of  $u_d^0$ . This ratio increases with  $Y_{VL}^0$ , has a negligible dependence upon the solvent identity and is independent upon the solute identity. The fact that this ratio is always smaller than  $Y_{VL}^0/(1 - Y_{VL}^0)$  indicates that eventually there is a steady-state situation that establishes where the amount of fuel escaping through the cluster boundary balances that evaporating from the drops.

Plots of the respective ratios (all at  $RI = 0.05$ ) of the burned fraction during external cluster combustion to the fraction that escaped the cluster for solvent,  $f_{b,s}/f_{loss,s}$ , and for solute,  $f_{b,v}/f_{loss,v}$ , depicted in Figs. 10 and 11 show two types of behavior. Strong flames that establish further away from the cluster surface (see Fig. 12 displaying the nondimensional distance from flame to cluster) are encountered for smaller  $\Phi^0$ 's and for larger  $u_d^0$ 's. In this case, it is only a small fraction of the fuel released from the cluster that is burned by the time of drop disappearance. For large  $u_d^0$ 's, the small evaporation rate at the end of the drop lifetime can no longer sustain the strong flame and instead of burning, extinction occurs. Mathematically, extinction is identified when the integrated consumption rate at the flame decreases instead of increasing with time. This means that a quasi-steady flame can no longer be maintained; it is possible that an unsteady flame could still exist under these conditions. Weak flames establish extremely close to the cluster surface; they occur mainly for large  $\Phi^0$ 's and small  $u_d^0$ 's. These flames behave asymptotically like classical quasi-steady diffusion flames where the fuel emitted by the cluster is almost entirely burnt in the flame ( $f_{b,s}/f_{loss,s}$  and  $f_{b,v}/f_{loss,v}$  are nearly 1). For intermediary values of  $u_d^0$ , the classical behavior of the diffusion flame is never reached, indicating the importance of convective effects. Note that  $f_{b,v}/f_{loss,v} \geq f_{b,s}/f_{loss,s}$ , with the equality occurring for weak diffusion flames. In that case, convective effects which preferentially evaporate the solute are not important. Examination of  $f_{loss,v}/f_{loss,s}$  shows that it is only a very slightly increasing function of  $\Phi^0$  and depends mainly upon  $Y_{VL}^0$  and  $u_d^0$ . This ratio depends only slightly upon solvent identity and does not depend upon solute identity. A similar comment applies to  $f_{b,v}/f_{b,s}$ , except that instead of it being a slightly increasing function of  $\Phi^0$  it is a slightly decreasing function of  $\Phi^0$ . Thus, although proportionally less solute is released from the cluster for small  $\Phi^0$ , proportionally a larger fraction of solute is burned. The situation where extinction is obtained represents an exception, as both ratios are increasing functions of  $\Phi^0$ .

For diffusion-dominated combustion, the fraction of fuel burnt during combustion is an increasing function of  $\Phi^0$  because ignition occurs earlier during the drop lifetime. As convective effects become important, the flame is relatively stronger in the small  $\Phi^0$  regime than in the purely diffusion regime as evidenced by the slope of the nondimensional flame distance to the cluster surface; as a result, it burns a larger fraction of fuel. Thus, for intermediary convective combustion, the fuel fraction burned during combustion is a nonmonotonic function of  $\Phi^0$ , and convex. When convection dominates, the flame is considerably stronger for small  $\Phi^0$ 's and accordingly an increasing fuel fraction is burned. The total fraction of fuel burned (flash flame and combustion) is an increasing function of  $\Phi^0$  since the later ignition for small  $\Phi^0$ 's also corresponds to situations where there is less oxygen inside the cluster and thus less fuel may be consumed by the flash flame.

Changing the ignition kinetics translates and enlarges or shrinks the collective flame regime on the  $\Phi^0$  axis but does not change the results qualitatively.

### 3 QUIESCENT, SUBCRITICAL AND SUPERCRITICAL EVAPORATION OF $LO_x$ DROPS IN CLUSTERS: MODELING

It is well known that, at supercritical pressures, the entities which were drops of  $LO_x$  at subcritical pressures no longer maintain their surface as the surface tension becomes null; thus, the previous models describing behavior at atmospheric pressure no longer apply at supercritical pressures. In this writing, the entities which were drops at subcritical conditions are still assumed to be spherical at supercritical conditions and shall be called "pseudodrops". Since the surface tension is a decreasing function of pressure, the drop surface does not vanish suddenly at the critical point but instead there are gradual variations in the state of  $LO_x$  drops as a function of pressure.

Current models of single, isolated, supercritical pseudodrop behavior<sup>11, 12</sup> retain the subcritical classical formalism, including the assumption of thermodynamic equilibrium at the drop surface, while incorporating the new aspects of volubility, binary-fuel, non ideal gas equations of state. The assumption is made that the drop surface suddenly vanishes when the supercritical point is attained. Presented below are aspects of a new model of subcritical drop and supercritical pseudodrop evaporation that takes another approach to the modeling of this very complex problem: (1) the difficulty of the vanishing surface tension is bypassed by writing the conservation equations for a general binary fluid system, (2) the equations of state are exact in the sense that they are those experimentally measured at relatively low temperatures compared to those prevailing during combustion, and are further extended to high temperatures using thermodynamically accepted concepts, and (3) evaporation is not constrained to be an equilibrium process. The equation of state determines the phase of the system (through the number of molar volume roots). For example, if the pressure is atmospheric and the density is  $O(1) \text{ g/cm}^3$ , then the compound is in the liquid state. One expects that in this case the surface acts as a discontinuity for the mass fraction profiles. However, in the general case where a liquid no longer exists, the mass fraction transition profiles are not expected to have sharp gradients across the boundary.

#### 3.1 Conservation equations

The conservation equations are written in the most general form using partial molar fluxes and the heat flux to describe phenomena related to nonequilibrium gas dynamics as applied to binary mixtures. After considerable algebra, it is found that these equations are as follows:

-continuity

$$\frac{\partial \rho}{\partial t} + \frac{\partial(\rho u_\beta)}{\partial x_\beta} = 0 \quad (1)$$

where  $\rho$  is the density,  $t$  is the time,  $x_\beta$  are the coordinates, and  $u_\beta$  are the velocities; the conventional index notation for expressing derivatives and sums apply.

-momentum conservation equation (the  $\alpha$  direction)

$$\frac{\partial(\rho u_\alpha)}{\partial t} + \frac{\partial(\rho u_\alpha u_\beta)}{\partial x_\beta} + \frac{\partial p}{\partial x_\alpha} = \frac{\partial \tau_{\alpha\beta}}{\partial x_\beta} \quad (2)$$

where  $p$  is the pressure and  $\tau_{\alpha\beta} = \eta[(\partial u_\alpha / \partial x_\beta - \partial u_\beta / \partial x_\alpha) - (2/3)\delta_{\alpha\beta} \partial u_\gamma / \partial x_\gamma]$  is the stress tensor in which  $\eta$  is the mixture viscosity and  $\delta_{\alpha\beta}$  is a tensor having unit diagonal, its other components being aul].

-species conservation

For a binary mixture one obtains

$$\frac{DX_1}{Dt} - \frac{m}{m_2 n} \nabla \cdot \vec{J}_1 = -\frac{DX_2}{Dt} \quad (3)$$

where  $DX_1/Dt \equiv \partial X_1/\partial t + u_\beta \partial X_1/\partial x_\beta$ ,  $X_1 = m_2 Y_1 / [m_1 + (m_2 - m_1) Y_1]$  is the mole fraction of species 1,  $Y_1$  is the mass fraction of species 1,  $m$  is the molar mass,  $m_i$  is the partial molar mass of species  $i$ ,  $n$  is the total number of moles per unit volume, and  $\vec{J}_i$  is the molar flux of species  $i$ . Using thermodynamic relationships and introducing a mutual diffusion coefficient,  $D_m = L_{11} (m/m_2)^2 V / (X_1 X_2)$  where  $L_{11}$  is one of the coefficients of the transport matrix<sup>13</sup> (relating fluxes to thermodynamic driving forces) proportional to Fick's term and  $V$  is the molar volume, and a ratio between the thermal and mutual diffusivities,  $k_T = (L_{1q}/L_{11}) \beta m_2/m$ , where  $L_{1q}$  is the coefficient of the transport matrix proportional to the Soret term,  $\beta = 1/(R_u T)$  where  $R_u$  is the universal gas constant and  $T$  is the temperature, one can calculate  $\vec{J}_1$  to be

$$\vec{J}_1 = -(m_2/m) (\vec{J}_b + X_1 X_2 k_T n D_m \nabla \ln T) \quad (4)$$

where

$$\vec{J}_b = n D_m \{ \alpha_D \nabla X_1 + \beta [m_1 m_2 X_1 X_2 / m] [(V_1/m_1 - V_2/m_2) \nabla p + (h_2/m_2 - h_1/m_1) \nabla \ln T] \} \quad (5)$$

in which  $h_1$  and  $h_2$  are partial molar enthalpies and  $\alpha_{Di} = 1 + \sum_{j \neq i} \gamma_j / \partial X_i$ ,  $\gamma_i$  being the activity coefficient of species  $i$  and  $\alpha_D = \alpha_{D1} = \alpha_{D2}$  according to the Gibbs-Duhem relationship.

-conservation of energy

The enthalpy equation combined with thermodynamic relationships for binary mixtures yields

$$\rho C_p \frac{M}{Dt} = \alpha_v T \frac{Dp}{Dt} - \nabla \cdot \vec{q} + \Phi_v + m_1 (h_1/m_1 - h_2/m_2) \nabla \cdot \vec{J}_1 \quad (6)$$

where  $\alpha_v = (\partial V/\partial T)_{p, X_1} / V$  is the thermal expansion ratio,  $\Phi_v = \tau_{\alpha\beta} \partial u_\alpha / \partial x_\beta$  is the viscous dissipation, and  $\vec{q}$  is the heat flux given by

$$\vec{q} = -(k_T R_u T) \vec{J}_b - k \nabla T \quad (7)$$

where consistent with the previous definitions  $k = \beta L_{qq} / T$  is the heat conductivity of the mixture.

## 3.2 Boundary conditions

Boundary conditions must be applied at three different locations: the drop or pseudodrop center, the interface which is initially the surface between the drop and the fluid, and the edge of the sphere of influence. At the center of each entity, spherical symmetry conditions prevail, whereas at the edge of the sphere of influence known conditions apply. These conditions may either be specified or be the result of calculations from a global system model paralleling the approach taken in subcritical studies<sup>5,14</sup>. The conditions at the interface express not only conservation of mass, species, momentum and energy, but also nonequilibrium evaporation and solvation.

Quantities are denoted with a subscript  $b$  to indicate that a quantity is evaluated at the interface. Initially,  $LO_x$  exists for  $r < R$  and the superscript  $L$  is used for this part of the space. At  $t = 0$ , fluid  $H_2$  surrounds the drop and thus the superscript  $G$  is used for  $r > R$ ,

Simple accounting of unknowns at the interface yields nine quantities: the velocities on the two sides of the interface,  $u_b^L$  and  $u_b^G$ ; the molar fraction of one of the compounds on the two sides of the interface,  $X_{1b}^L$  and  $X_{1b}^G$ ; the density on the two sides of the interface,  $\rho_b^L$  and  $\rho_b^G$ ; the drop or pseudodrop radius,  $R$ ; the temperature,  $T_b$ ; and the pressure,  $p_b$ . These nine unknowns can be calculated from the following nine relationships: the equation of state; conservation of mass; conservation of species; conservation of momentum; conservation of energy; continuity of specie flux; the evaporation law and continuity of surface heat flux; relationship between the regression rate and the mass emission flux,  $F_{ems}$ ; and a relationship between the mass emission flux and the mass fluxes on the two sides of the interface. While some of these conservation statements are classical, others are novel to this formulation and thus will be described below.

-mass balance at  $r = R$

$$u_b^G = u_b^L \rho_b^L / \rho_b^G - (\rho_b^L / \rho_b^G - 1) dR/dt \quad (8)$$

-heat balance at  $r = R$

$$A_d(q_{r,b}^G - q_{r,b}^L) = \{[h_2^G + (h_1^G - h_2^G)X_{1b}^G]/m^G - [h_2^L + (h_1^L - h_2^L)X_{1b}^L]/m^L\} dm_d/dt \quad (9)$$

where  $h_j^G = h_j(p_b, T_b, X_{1b}^G)$ ,  $h_j^L = h_j(p_b, T_b, X_{1b}^L)$  and  $h_1^G - h_1^L$  is the heat of evaporation whereas  $h_2^G - h_2^L$  is the heat of solution;  $A_d$  denotes the surface of the drop or pseudodrop,  $m_d$  denotes its mass and  $q_{r,b}$  represents the radial component of the heat flux.

-nonequilibrium evaporation law

By definition  $F_{ems} \equiv -(1/A_d) dm_d/dt$ . Calculating the fluxes at the molecular level, one obtains

$$F_{ems} = \sum_{j=1,2} [\alpha_{cj} m_j u_{Tj} (n_{j,equil}^G - n_j^G)] \quad (10)$$

where  $\alpha_{cj}$ 's are accommodation coefficients,  $n_{j,equil}^G$ 's can be calculated from thermodynamic relationships and  $u_{Tj}$  is the mean normal velocity of a molecule of species  $j$  due to thermal fluctuations.  $u_{Tj}$  can be calculated for a pure liquid from Eyring's theory<sup>15</sup>; no method exists, however, to calculate this velocity for a general fluid,

-continuity of specie 1 flux at  $r = R$

$$m_1 (J_{1r,b}^G - J_{1r,b}^L) = (Y_{1b}^L - Y_{1b}^G) F_{ems} \quad (11)$$

where  $J_{1r,b}$  represents the radial component of the mass flux of specie 1.

### 3.3 Calculation of state functions

The validity of determining state functions using simple polynomial equations, such as the Peng-Robinson (P-R) equation of state (eos), is questionable given the fact that the compressibility factor is invariant with the compound; a statement that is physically incorrect. On the other hand, experimentally determined eos's do not cover the range of high temperatures relevant to evaporation and combustion processes; also no mixing rules have been developed for exact eos's. Therefore, new strategies are needed to find reliable eos's. The concept described below is simple yet powerful because it yields precisely reliable eos's.

For a pure component the enthalpy,  $H$ , can be considered to be the sum of two terms:  $(H - H^0)$  and  $H^0$  which is the enthalpy at a reference state.  $H - H^0$  is a departure function from an ideal gas which can be calculated using the P-R eos<sup>16</sup>, and  $H^0$  can be curve fitted to agree faithfully with experimentally measured eos's. Since values of

$H^0$  are measured only at relatively low pressures and temperatures compared to those of combustion, the estimate of  $H^0$  is improved by extrapolating a curve fit beyond the experimentally measured values. This is accomplished by calculating  $H^0$  as the sum of experimentally measured values,  $H$ , and the departure function,  $H - H^0$ , and further extrapolating the resulting value of  $H^0$ . This procedure allows the calculation of state functions for pure compounds. Figure 13 shows  $H^0$  for hydrogen obtained with this procedure. Further, according to Prausnitz et al.<sup>16</sup>, standard mixing rules for the P-R eos combined with simple linear mixing of reference state values can be used to calculate the mixture enthalpy and thus eos.

### 3.4 Numerical difficulties specific to the model

The model presented above yields a set of equations that is extremely stiff. The stiffness is introduced primarily by the nonequilibrium evaporation law at the drop surface. Experience with the code shows that  $\tau_{eff}$  is very sensitive to the values of the mass fractions and temperature at the surface. Various strategies are being implemented to mitigate this difficulty. A baseline solution is expected in the near future.

### 3.5 Drop interactions at supercritical conditions

Although results from the above model are not yet available, based upon previous experience with models of drop interactions at subcritical conditions one may speculate about the importance of drop interactions at supercritical conditions. At these higher pressures, the density ratio between the fluid in the drop and that in the surroundings is no longer  $O(10^{-3})$  but instead becomes  $O(1) - O(10^2)$ . This indicates that the coupling between drops and surroundings will be stronger which implies that thermodynamic drop interactions will be more important. Thus, it is expected that dense cluster effects may become apparent at larger  $\Phi^0$ 's than in subcritical conditions.

## 4 SUMMARY/AND FUTURE DIRECTIONS

The supercritical conditions prevailing in liquid rocket engine combustion chambers present a formidable modeling challenge. In particular, multicomponent fuel aspects combined with supercritical aspects need to be understood in the context of multidrop interactions. The models presented above represent only a step in the task of modeling the liquid rocket configuration. If the combustion chamber is considered to represent the macroscale, one may define the microscale as that which is much smaller than the macroscale (for example by a factor  $10^3$ ). To proceed toward modeling the entire combustion chamber, it is first envisaged that a spray model will be built using cluster models as microscale models. Further, these individual spray models will have to be combined in the multi-spray configuration of the liquid rocket combustion chamber. At each step of development, experimental results are necessary to verify the validity of the models. So far, experimental results in supercritical conditions have been unavailable even for the limited configuration of a cluster of drops. Thus, clever experimental techniques will play a very important role in the development of accurate models.

## References

- <sup>1</sup> Harrje, D. T. and Reardon, F. H., "Liquid Propellant Rocket Combustion Instability", NASA SP-194, 1972

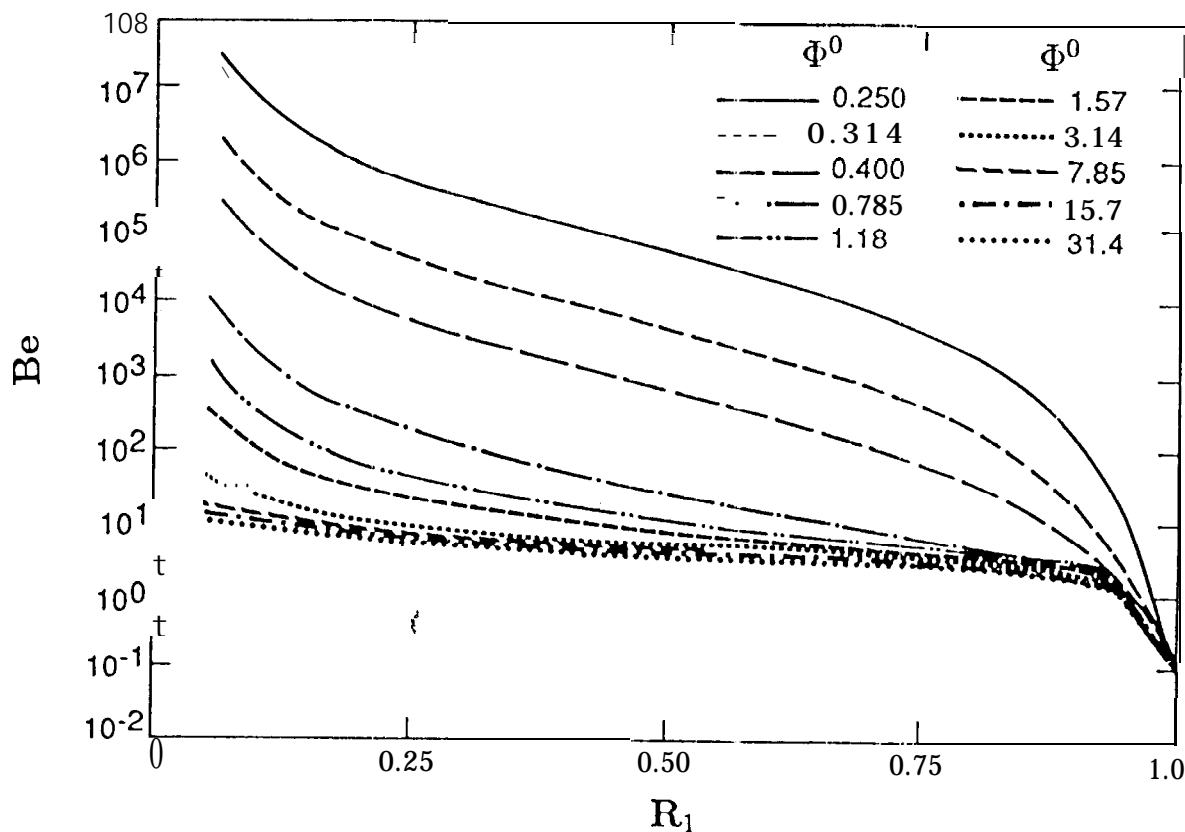
- <sup>2</sup>Gross, K., "Liquid Behavior at Critical and Supercritical Conditions", JANNAF Workshop, September 6, 1989, University of California Irvine, Ca.
- <sup>3</sup>Gross, K., personal communication, April 1990, Huntsville, Al.
- <sup>4</sup>Law, C. K., "Recent Advances In Droplet Vaporization and Combustion", *Prog. Energy Combust. Sci.*, Vol. 8, 1982, pp. 171-201
- <sup>5</sup>Bellan, J. and CutTel, R., "A Theory of Non-Dilute Spray Evaporation Based Upon Multiple Drop Interaction", *Combust. and Flame*, Vol. 51, No. 1, 1983, pp. 55-67
- <sup>6</sup>Harstad, K. and Bellan, J., "A Model of the Evaporation of Binary-Fuel Clusters of Drops", *Atomization and Sprays*, Vol.1, 1991, pp. 367-388
- <sup>7</sup>Bellan, J. and Harstad, K., "Ignition of Binary-Fuel Drops in Clusters", submitted for publication and in review
- <sup>8</sup>Law, C. K. and Chung, S. H., "An Ignition Criterion for Droplets in Sprays", *Combust. Sci. and Tech.*, Vol. 22, 1980, pp. 17-26
- <sup>9</sup>Bellan, J. and Harstad, K., "Ignition of Non-Dilute Clusters of Drops in Convective Flows", *Combust. Sci. and Tech.*, Vol. 53, 1987, pp. 75-87
- <sup>10</sup>Bellan, J. and Harstad, K., "Evaporation, Ignition and Combustion of Non Dilute Clusters of Drops", *Combust. and Flame*, Vol. 79, 1990, pp. 272-286
- <sup>11</sup>Yang, V., Lin, N. N. and Shuen, J. S., "Vaporization of Liquid Oxygen ( $LO_x$ ) Droplets at Supercritical Conditions", AIAA-92-0103, presented at the 30th Aerospace Sciences Meeting, Reno, NV., 1992
- <sup>12</sup>Delplanque, J-P. and Sirignano, W. A., "Transient Vaporization and Burning for an Oxygen Droplet at Sub- and Near-Critical Conditions", AIAA-91-0075, presented at the 29th Aerospace Sciences Meeting, Reno, NV., 1991
- <sup>13</sup>Peacock-Lopez, E. and Woodhouse, L., "Generalized Transport Theory and its Applications in Binary Mixtures", *Fluctuation Theory of Mixtures*, Matteoli, E. and Mansoori, G., Ed. Taylor and Francis, 1990
- <sup>14</sup>Bellan, J. and Harstad, K., "Turbulence Effects During Evaporation of Drops in Clusters", *Int. J. Heat Mass Transfer*, Vol.31, No. 8, pp. 1655-1668
- <sup>15</sup>Bird R., Stewart, W. and Lightfoot, E., "Transport Phenomena", John Wiley & Sons, 1960
- <sup>16</sup>Prausnitz, J., Lichtenthaler, R. and de Azevedo, E., "Molecular Thermodynamics of Fluid-Phase Equilibrium", Prentice-Hall, inc., 1986

#### ACKNOWLEDGMENT

The research described in this document has been conducted at the Jet Propulsion Laboratory, California Institute of Technology under sponsorship from the U.S. Department of Energy, Energy Conversion and Utilization Technologies and Advanced Industrial Concepts with Mr. M. Gunn, Jr. and Dr. G. Varga, respectively, serving as contract monitors, under an agreement with the National Aeronautics and Space Administration (NASA); and under sponsorship from NASA/Marshall Space Flight center with Mr. K. Gross serving as contract monitor.

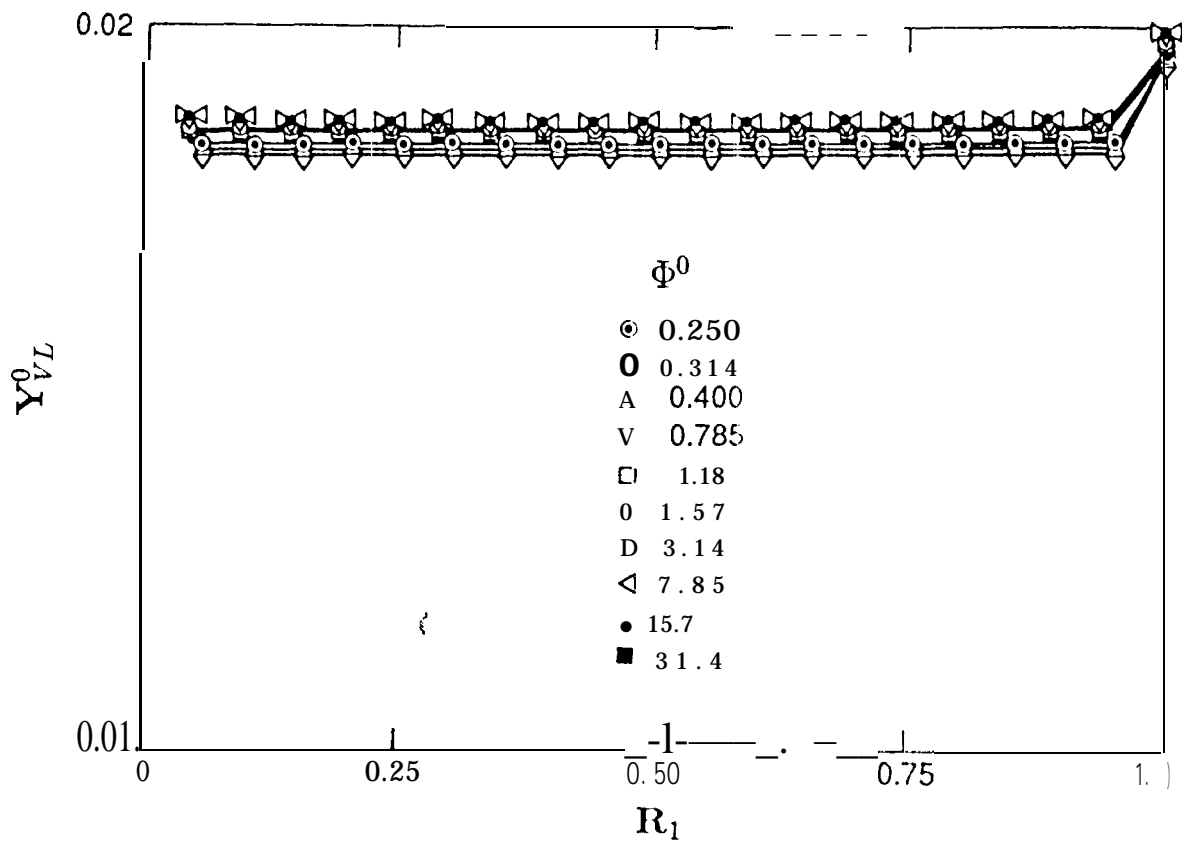
	solvent	solute	$u_d^{0, \gamma^0}$	$E_{ign}$	$kcal/mole$
+	n-decane	n-hexane	20 0.2	30 0.2	
□	n-decane	n-hexane	8 0	0.2	30
▽	n-decane	n-hexane	2 0 0	0.2	30
O	No. 2 GT	n-hexane	2 0	0.2	30
D	No. 2 GT	n-decane	2 0	0.2	30
A	No. 2 GT	n-decane	2 0	0.3	30
○	n-decane	n-hexane	2 0	0.2	28.5

Table 1. Parameters and symbols used in Figs. 7-12.



**Fig. 1 Variation of Be with the residual drop radius for several initial air/fuel mass ratios. The solvent is No. 2-GT oil, the solute is n-decane.**

$$T_{ga}^0 = 1000K, Y_{Fva}^0 = 0, T_{gs}^0 = 350K, Y_{V1}^0 = 0.02, u_d^0 = 200cm/s, R^0 = 2 \times 10^{-3}cm, R_c^0 = 3cm$$



**Fig. 2 Variation of the solute liquid mass fraction in the drop core with the residual drop radius for several initial air/fuel mass ratios. The initial conditions are those of Fig. 1.**

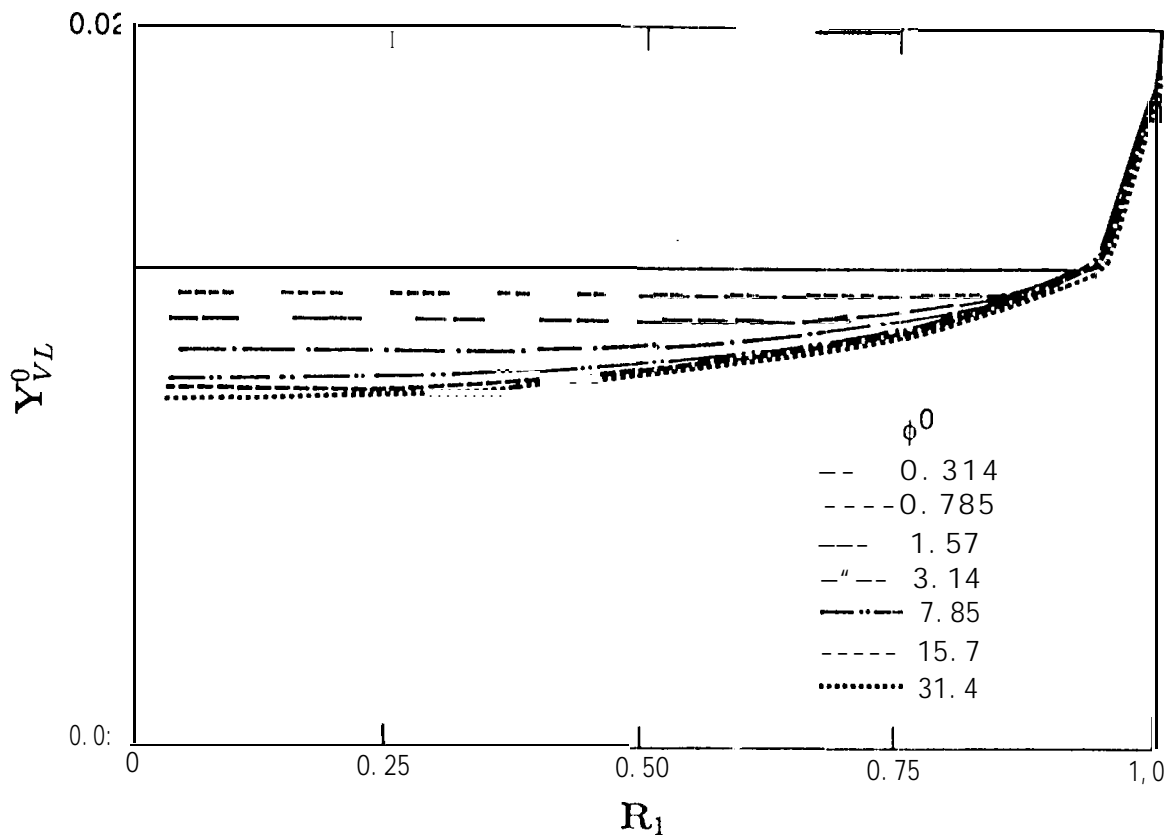


**Fig. 3 Variation of the solute liquid mass fraction in the drop core with the residual drop radius for several initial air/fuel, mass ratios. The solvent is No. 2-GT oil, the solute is n-decane.**

$$T_{ga}^0 = 1000K, Y_{Fva}^0 = 0, T_{gs}^0 = 350K, Y_{VL}^0 = 0.02, u_d^0 = 1000cm/s, R^0 = 2 \times 10^{-3}cm, R_c^0 = 3cm$$

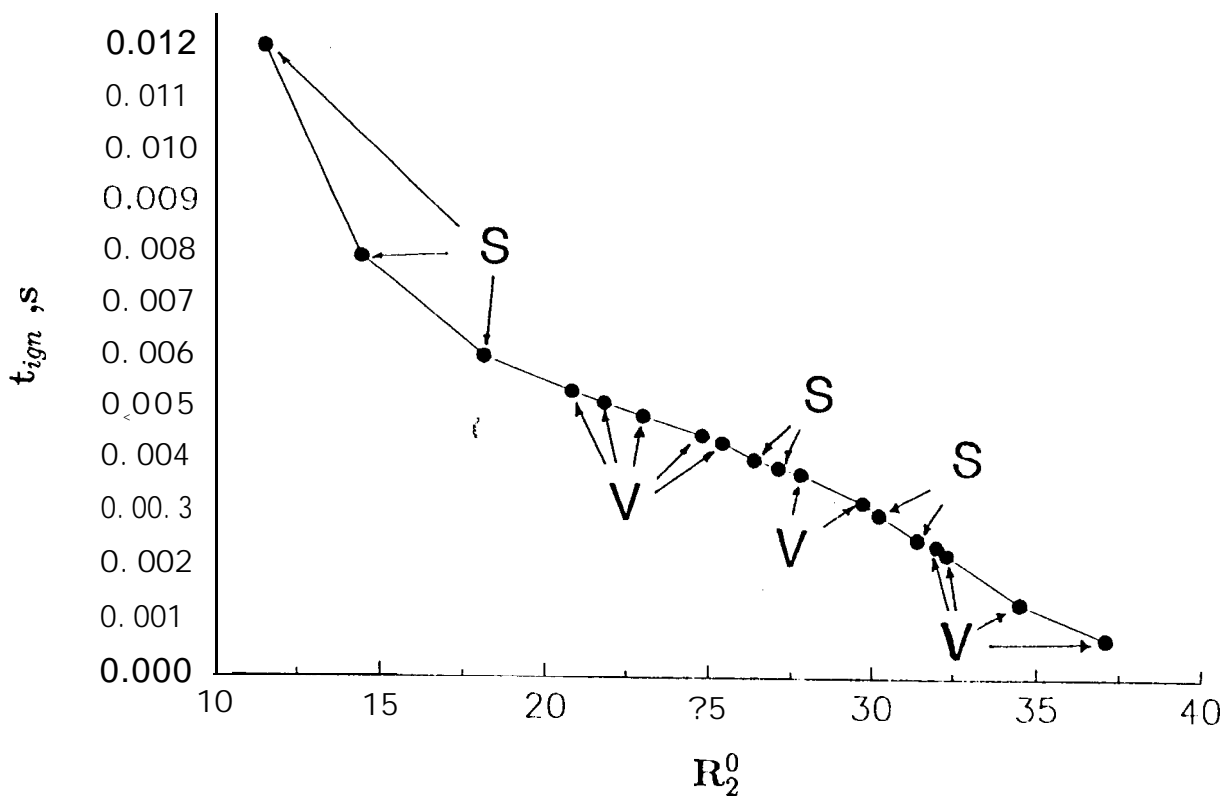


**Fig. 4 Ignition time versus the initial nondimensional radius of the sphere of influence. S designates solvent ignition; V designates solute ignition. The initial conditions are those of Fig. 1.**

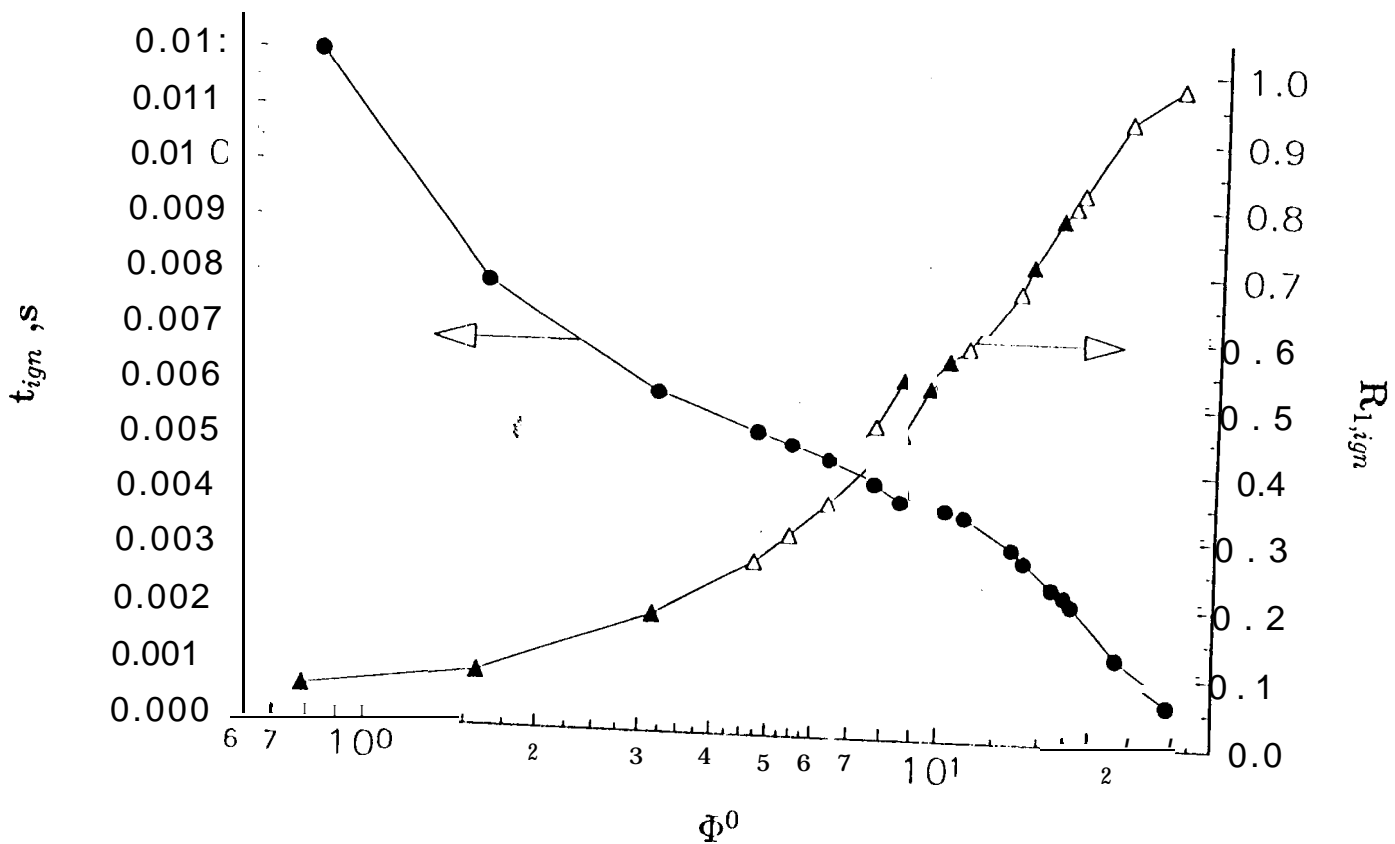


**Fig. 5 Ignition time and residual drop radius versus the initial air/ fuel mass ratio for the same initial conditions as in Fig. 1.**

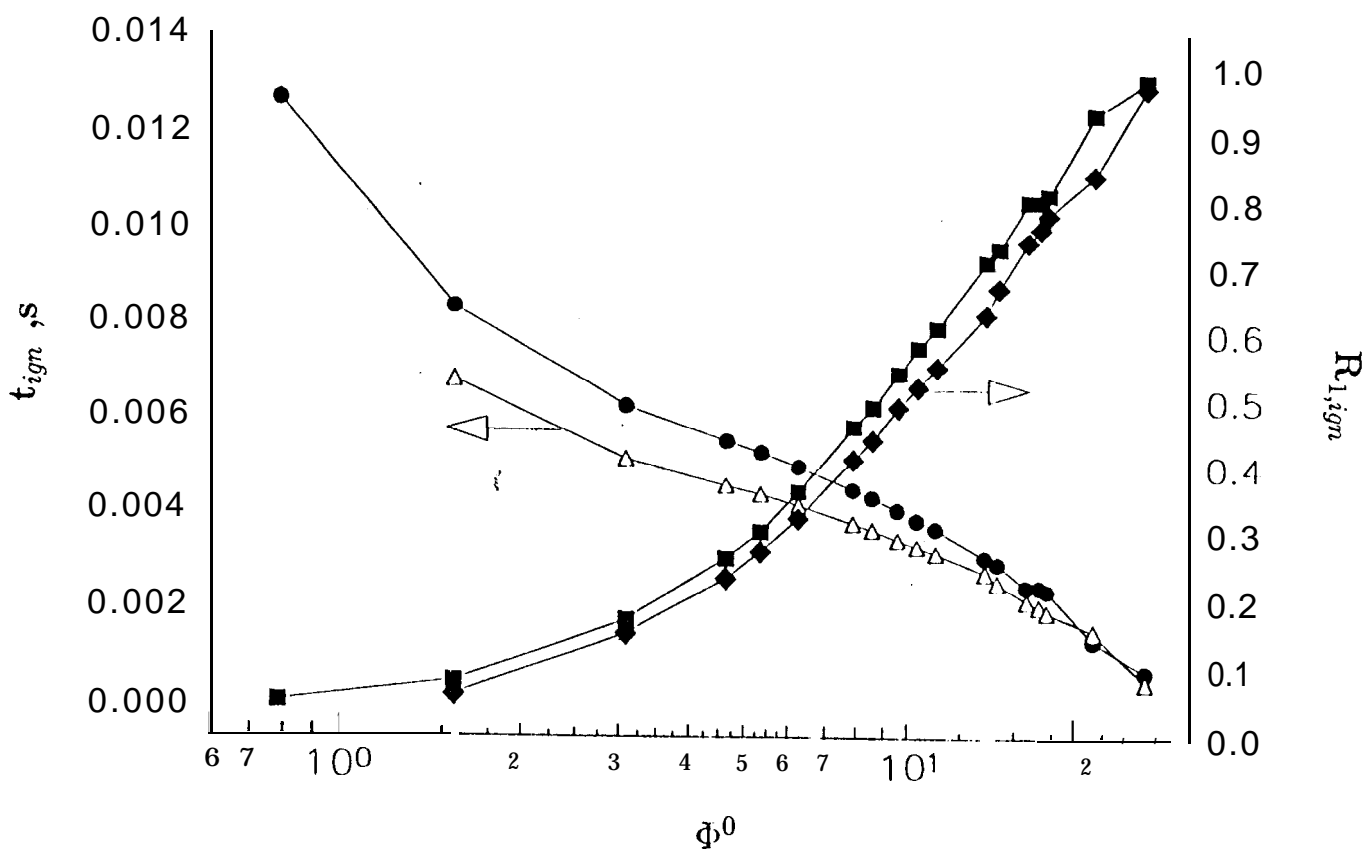


**Fig. 6 Ignition time and residual drop radius versus the initial air/fuel mass ratio for two binary fuels having hexane as the solute with  $Y_{VL}^0=0.2$ . The solvent is No. 2-GT oil for ● and ■ ; the solvent is n-decane for △ and ◆. The other initial conditions are those of Fig. 1.**

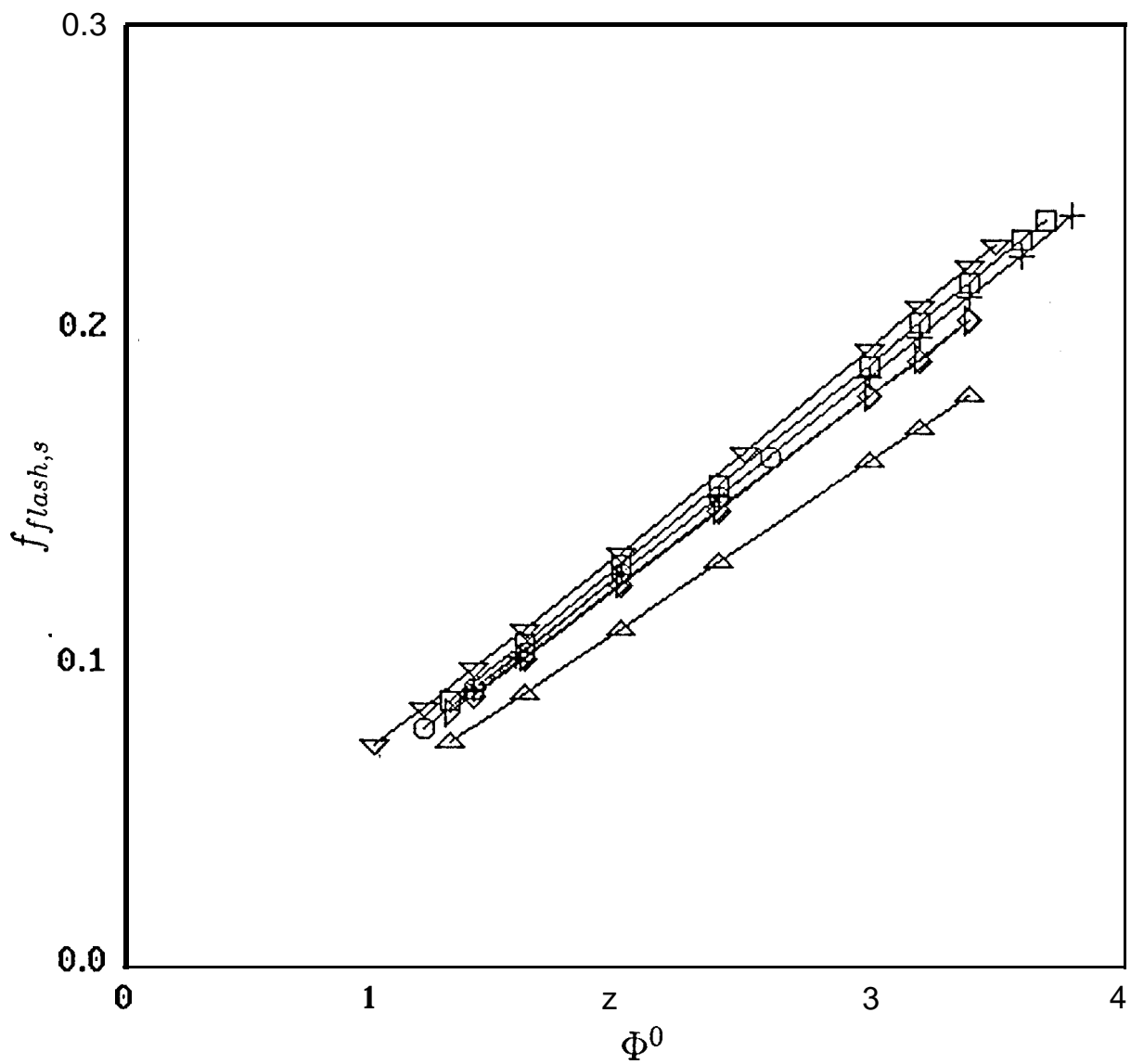


**Fig. 7** The solvent flash-flame burned fraction versus air/fuel mass ratio. The other initial conditions are those of Fig. 1.

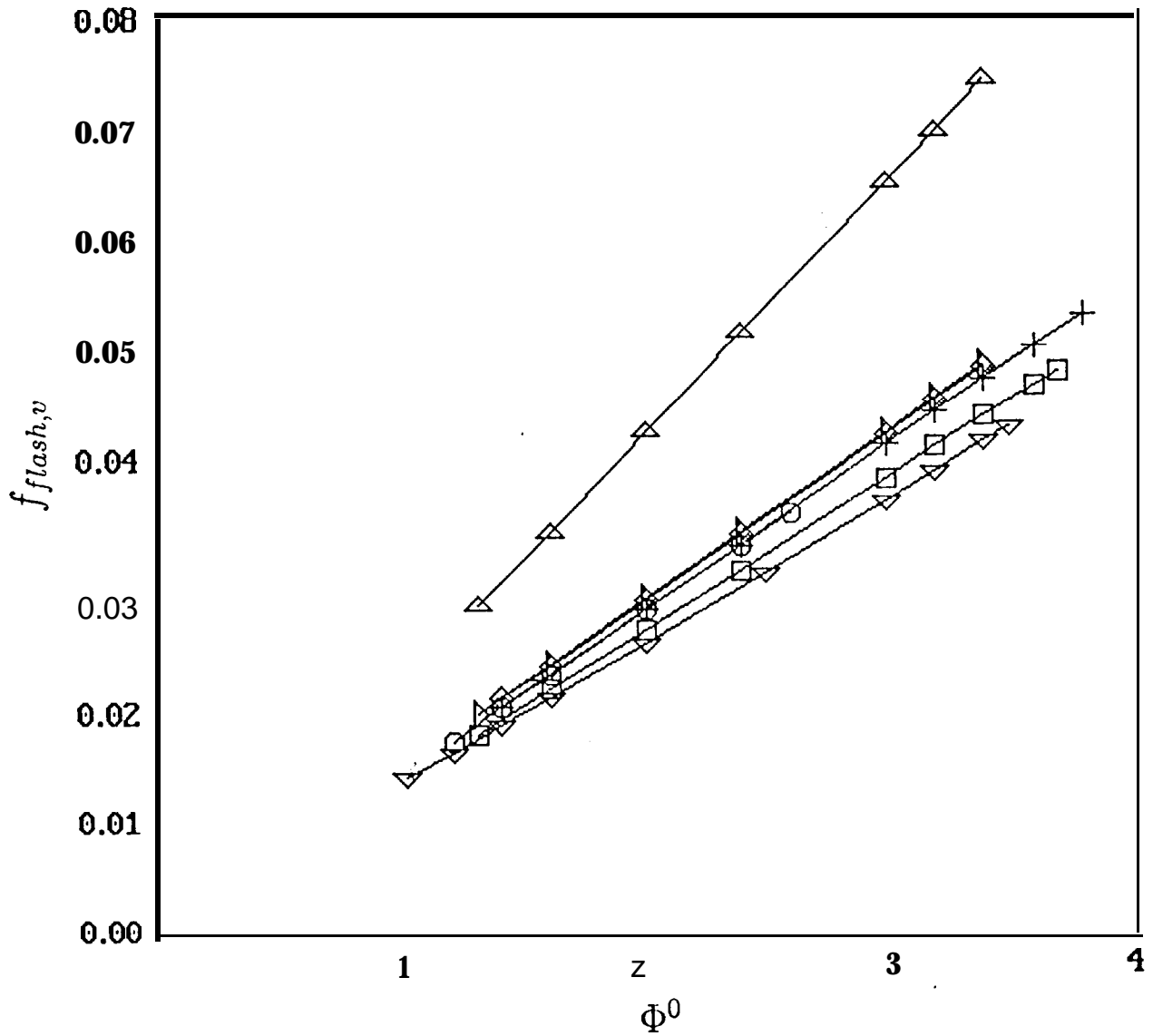


**Fig. 8** The solute flash-flame burned fraction versus air/fuel mass ratio. The other initial conditions are those of Fig. 1.

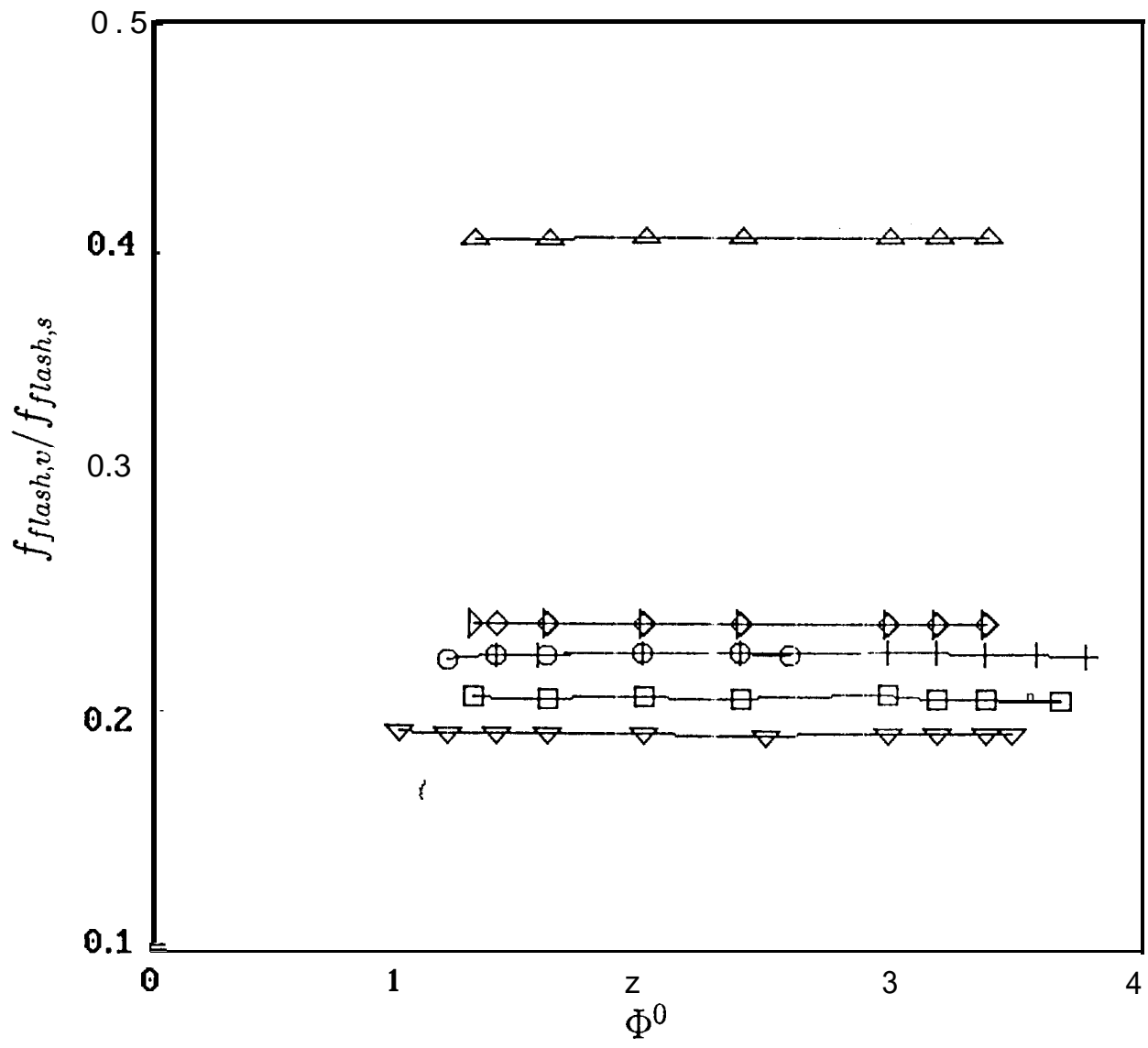


**Fig. 9 The ratio of flash-flame burned fractions versus air/fuel mass ratio. The other initial conditions are those of Fig. 1.**

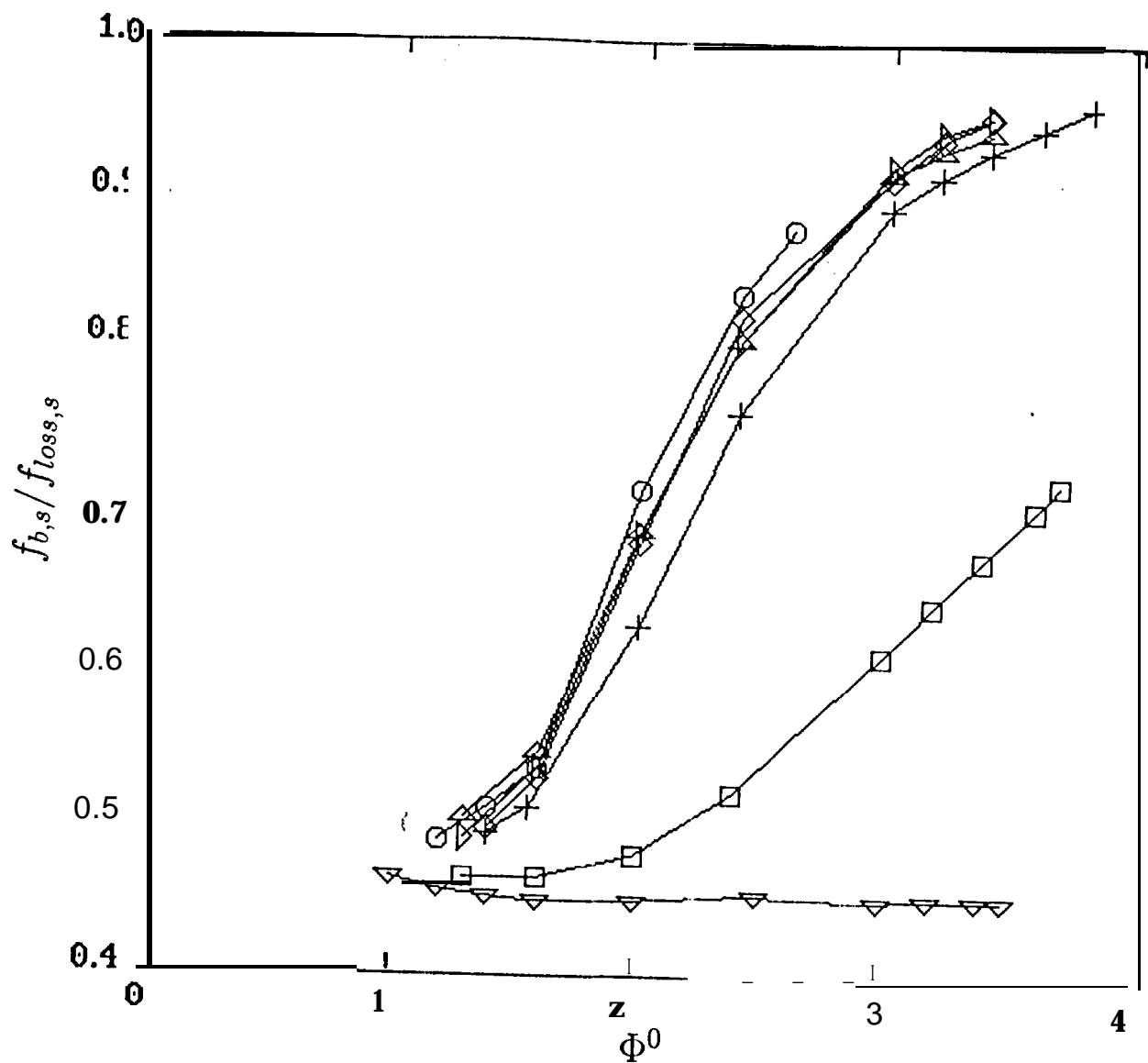


**Fig. 10** The ratio of lost to burned fractions for solvent versus air/fuel mass ratio. The other initial conditions are those of Fig. 1.

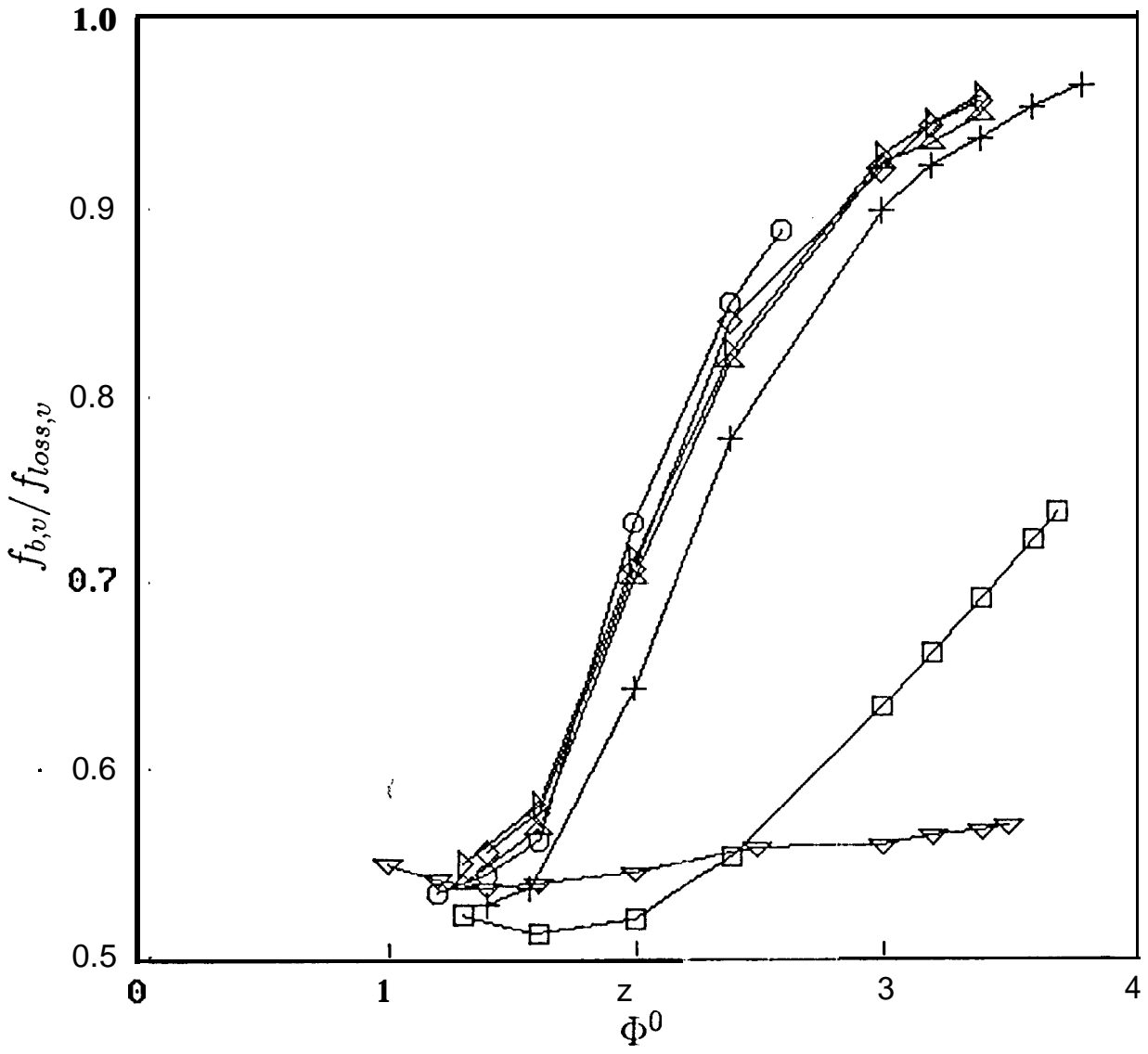


**Fig. 11 The ratio of lost to burned fractions for solute versus air/fuel mass ratio. The other initial conditions are those of Fig. 1.**

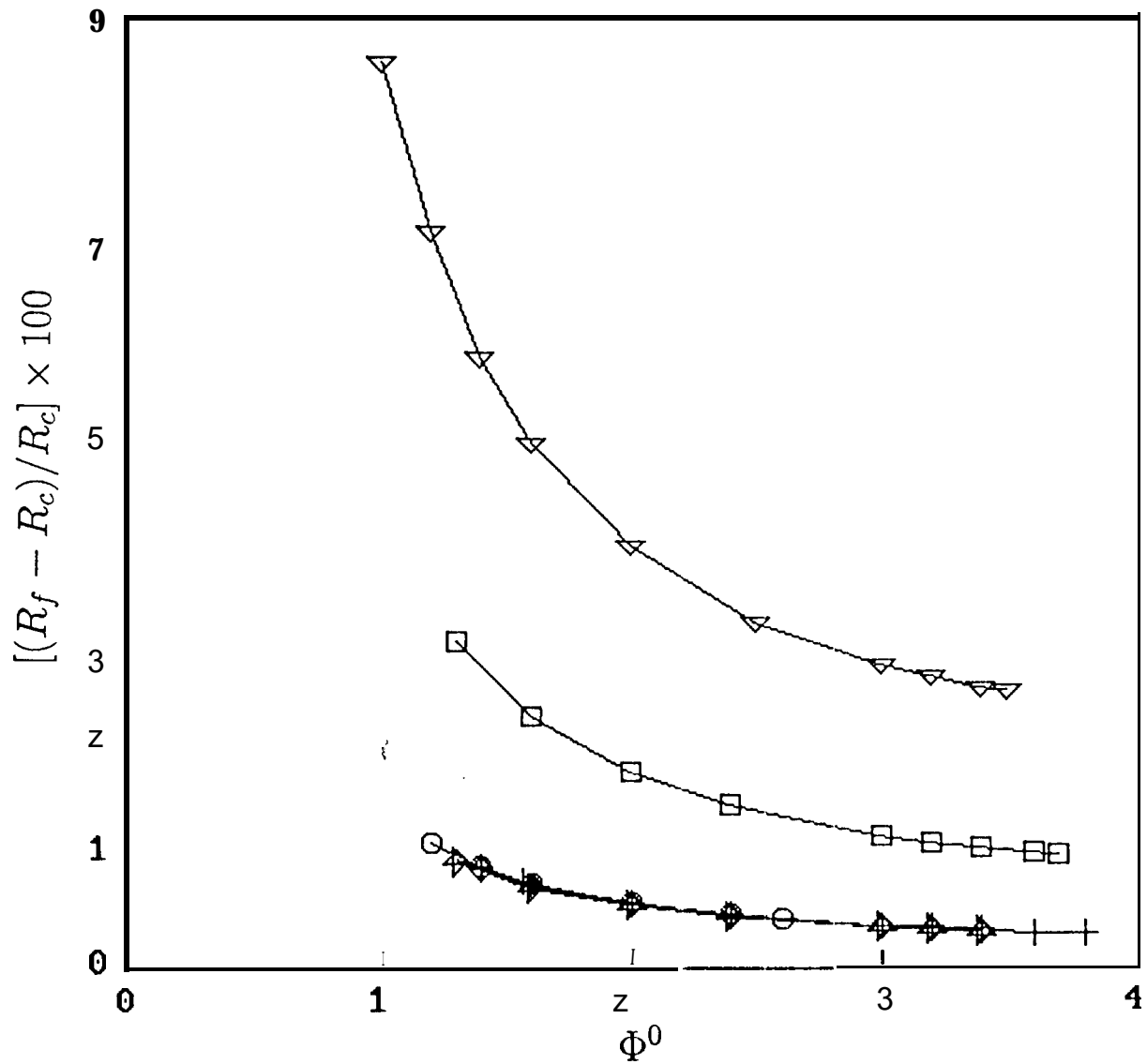


**Fig. 12 The nondimensional stand-off distance of the flame versus air/fuel mass ratio. The other initial conditions are those of Fig. 1.**

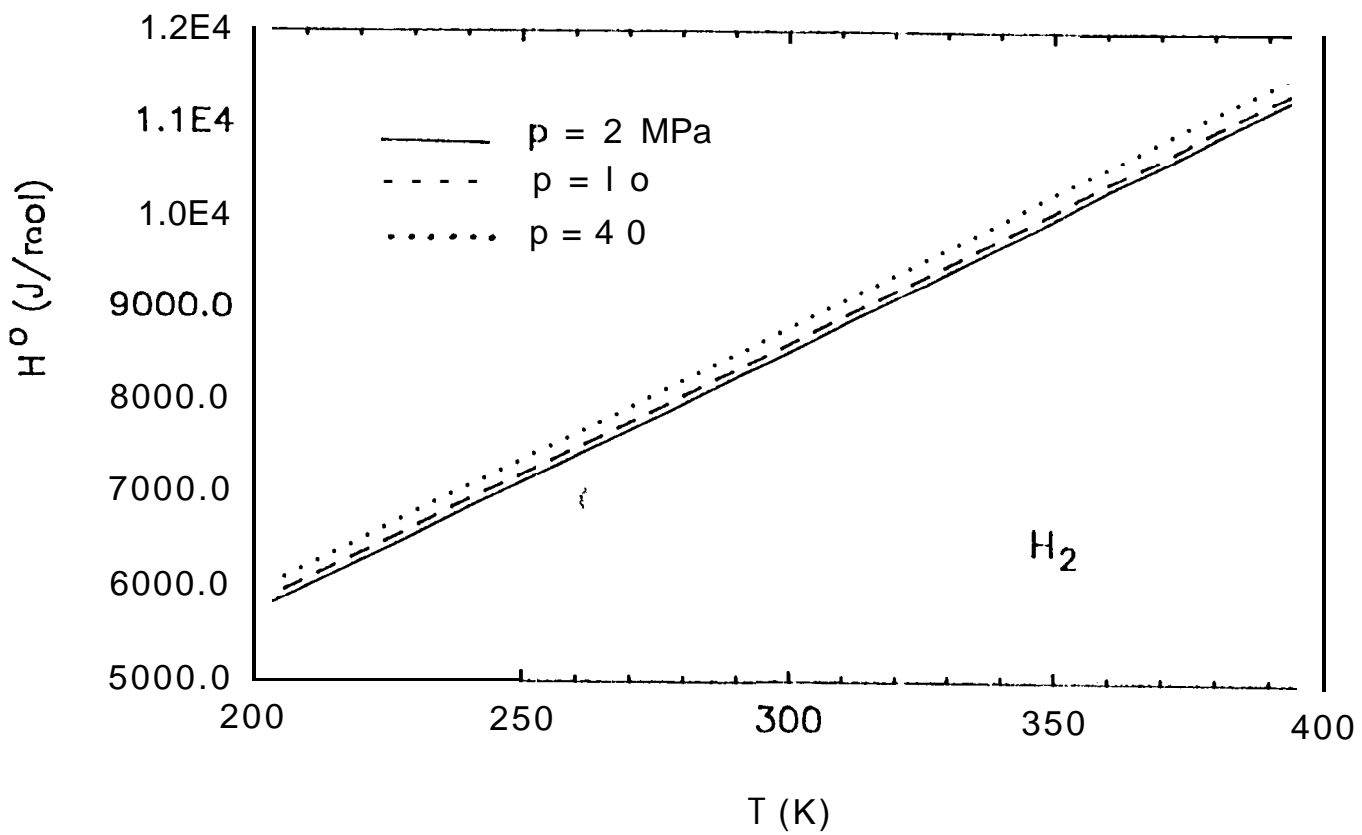


**Fig. 13 Variation of the enthalpy with the temperature for several pressures,**